

## Electronic Supplementary Information

# Morphology-controlled self-assembled nanostructures of complementary metalloporphyrin triads through intermolecular coordination tuning and their photocatalytic degradation for Orange II

Nirmal Kumar Shee and Hee-Joon Kim\*

*Department of Chemistry and Bioscience, Kumoh National Institute of Technology  
61 Daehak-ro, Gumi 39177, Republic of Korea*

## List of contents:

**Fig. S1**  $^1\text{H}$  NMR spectrum of triad **1** in DMSO- $d_6$ .

**Fig. S2**  $^1\text{H}$  NMR spectrum of triad **2** in DMSO- $d_6$ .

**Fig. S3**  $^1\text{H}$  NMR spectrum of triad **3** in DMSO- $d_6$ .

**Fig. S4**  $^1\text{H}$  NMR spectrum of triad **4** in DMSO- $d_6$ .

**Fig. S5**  $^1\text{H}$  NMR spectrum of triad **5** in DMSO- $d_6$ .

**Fig. S6**  $^1\text{H}$  NMR spectrum of triad **6** in DMSO- $d_6$ .

**Fig. S7** ESI-mass spectrum of triad **1**.

**Fig. S8** ESI-mass spectrum of triad **2**.

**Fig. S9** ESI-mass spectrum of triad **3**.

**Fig. S10** ESI-mass spectrum of triad **4**.

**Fig. S11** ESI-mass spectrum of triad **5**.

**Fig. S12** ESI-mass spectrum of triad **6**.

**Fig. S13** High-resolution FE-SEM images of the morphologies for self-assembled aggregates formed from the mixed solvent (toluene: *n*-hexane = 1:1). (a) **ZnP**; (b) **SnP**<sup>1</sup>.

**Fig. S14** Time-dependent absorption spectra of Orange II (ORII) in the presence of photocatalyst derived from triad **4** under visible-light irradiation.

**Fig. S15** Adsorption and desorption isotherms of  $\text{N}_2$  for catalyst **4** at 77 K.

**Fig. S16** Kinetics for the photocatalytic degradation of Orange II (ORII) by nanostructures derived from mixed solvent system under visible-light irradiation.

**Fig. S17** Catalytic cycles (consecutive 8 cycles) for photocatalyst **4** for the degradation of Orange II (ORII).

**Fig. S18** FE-SEM image of photocatalyst **4** after 8 consecutive cycles in the degradation of Orange II (ORII).

**Fig. S19** Performance of photocatalyst **4** (10 mg used) with respect to changes in initial concentration of Orange II (ORII).

**Fig. S20** Effect of temperature for the degradation by photocatalyst **4**.

**Fig. S21** Effect of pH of the solution for the degradation by photocatalyst **4**.

**Fig. S22** Photocatalytic degradation of Orange II (ORII) in aqueous solution by photocatalyst **4** generated from mixed solvent with the addition of different scavengers under visible light irradiation. **SnP**<sup>1</sup> and **ZnP** were also used as a catalyst for comparison.

**Fig. S23** ESI-mass spectrum (negative ion mode) of the reaction mixture of Orange II (ORII) with photocatalyst **4** after 1 h of visible-light irradiation.

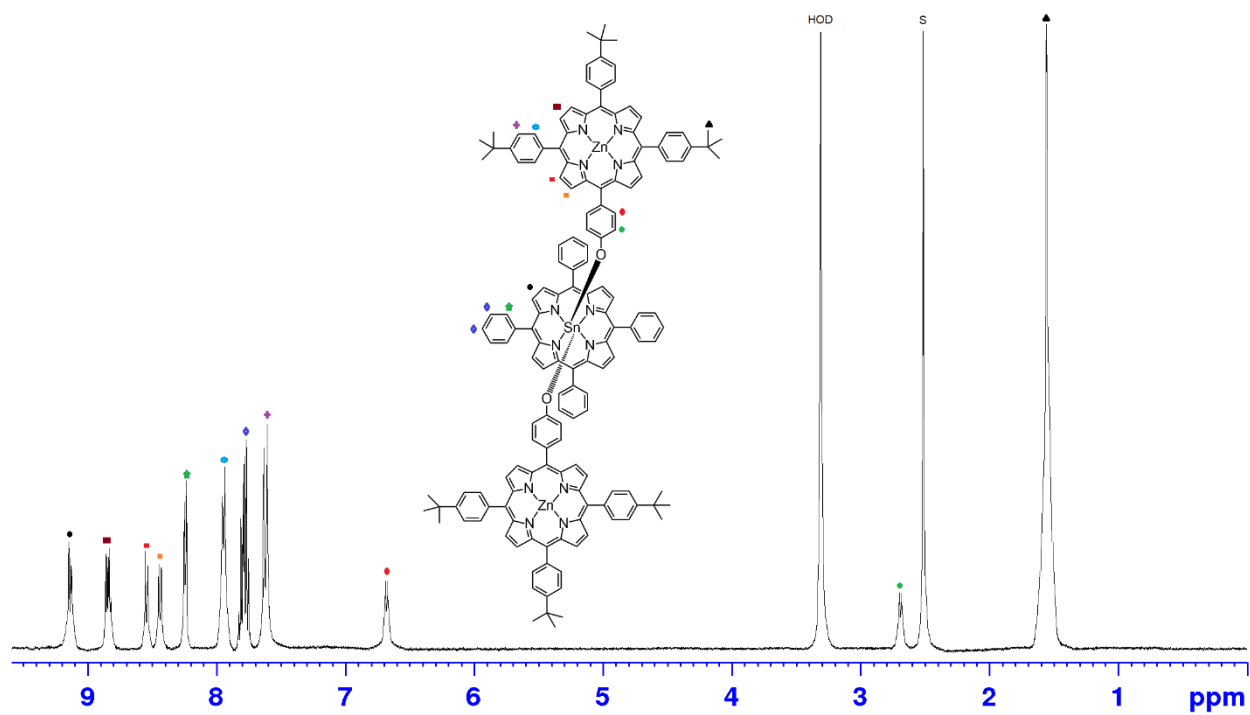


Fig. S1  $^1\text{H}$  NMR spectrum of triad **1** in  $\text{DMSO-d}_6$ .

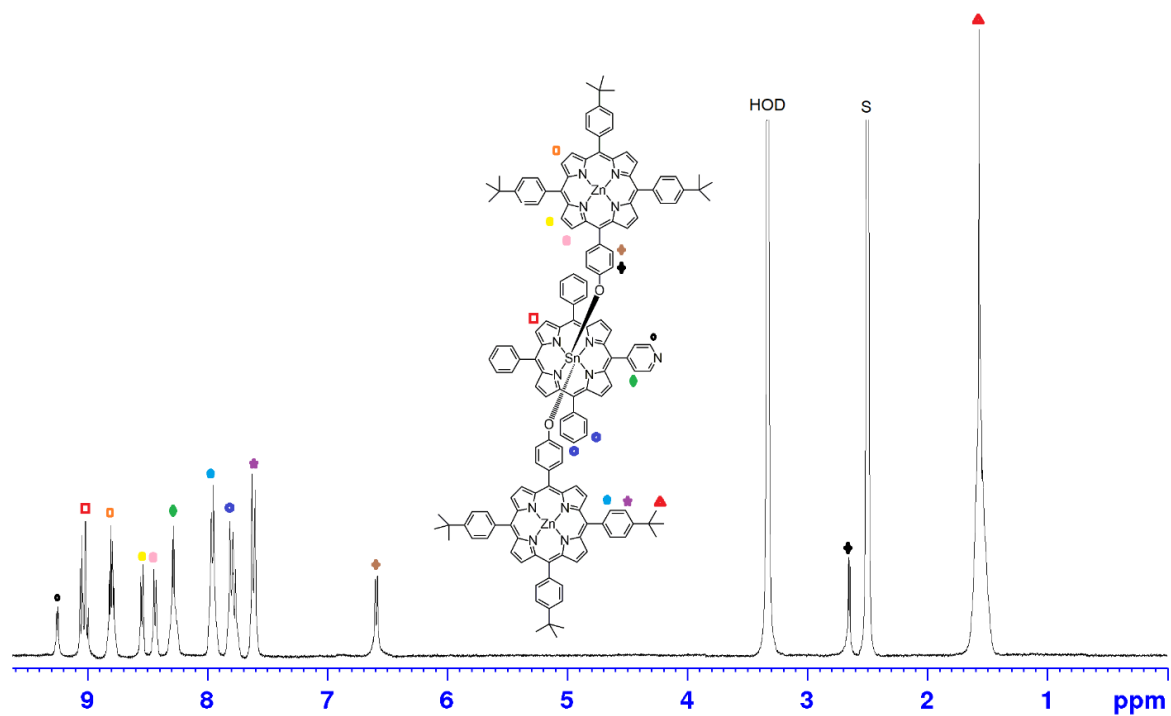


Fig. S2  $^1\text{H}$  NMR spectrum of triad **2** in  $\text{DMSO-d}_6$ .

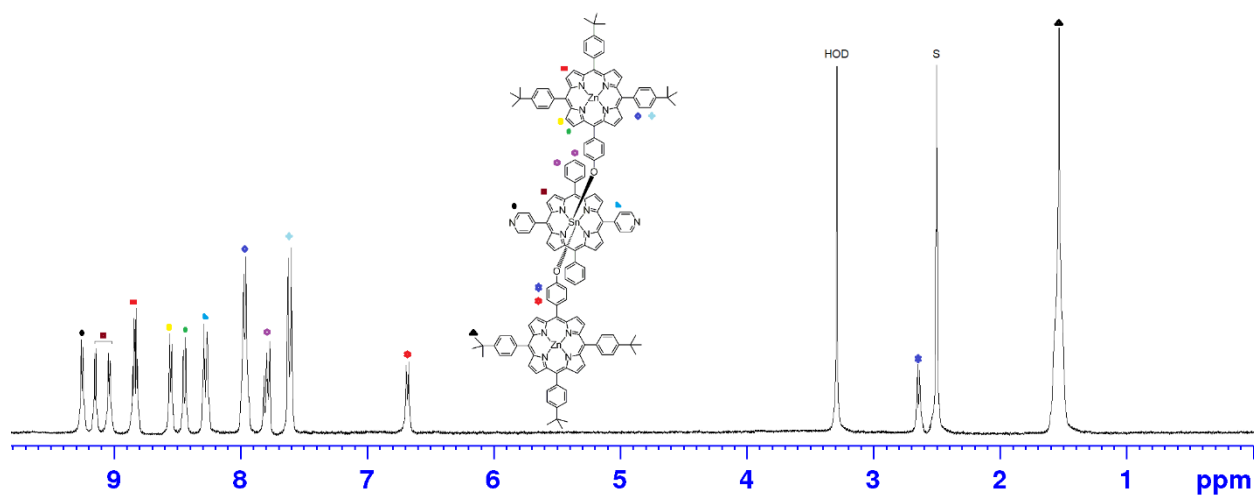


Fig. S3  $^1\text{H}$  NMR spectrum of triad 3 in  $\text{DMSO-d}_6$ .

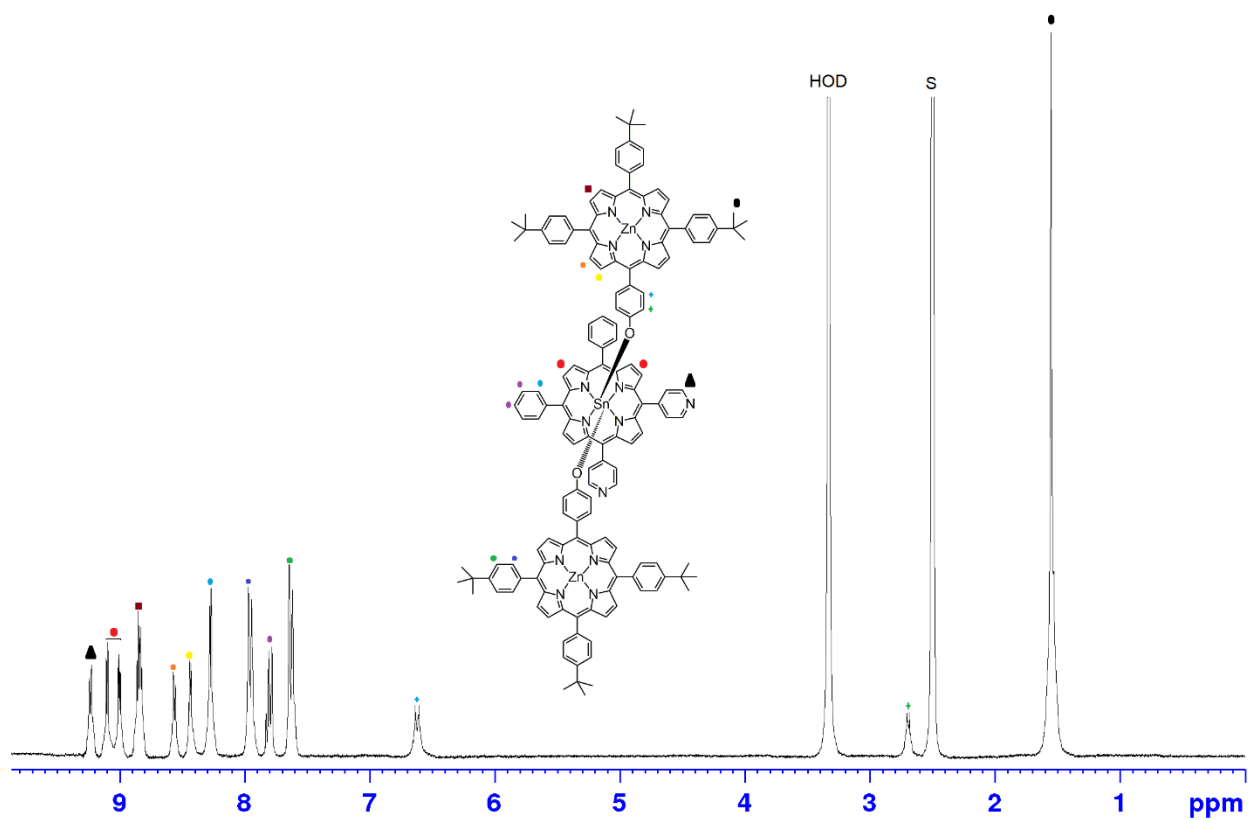


Fig. S4  $^1\text{H}$  NMR spectrum of triad 4 in  $\text{DMSO-d}_6$ .

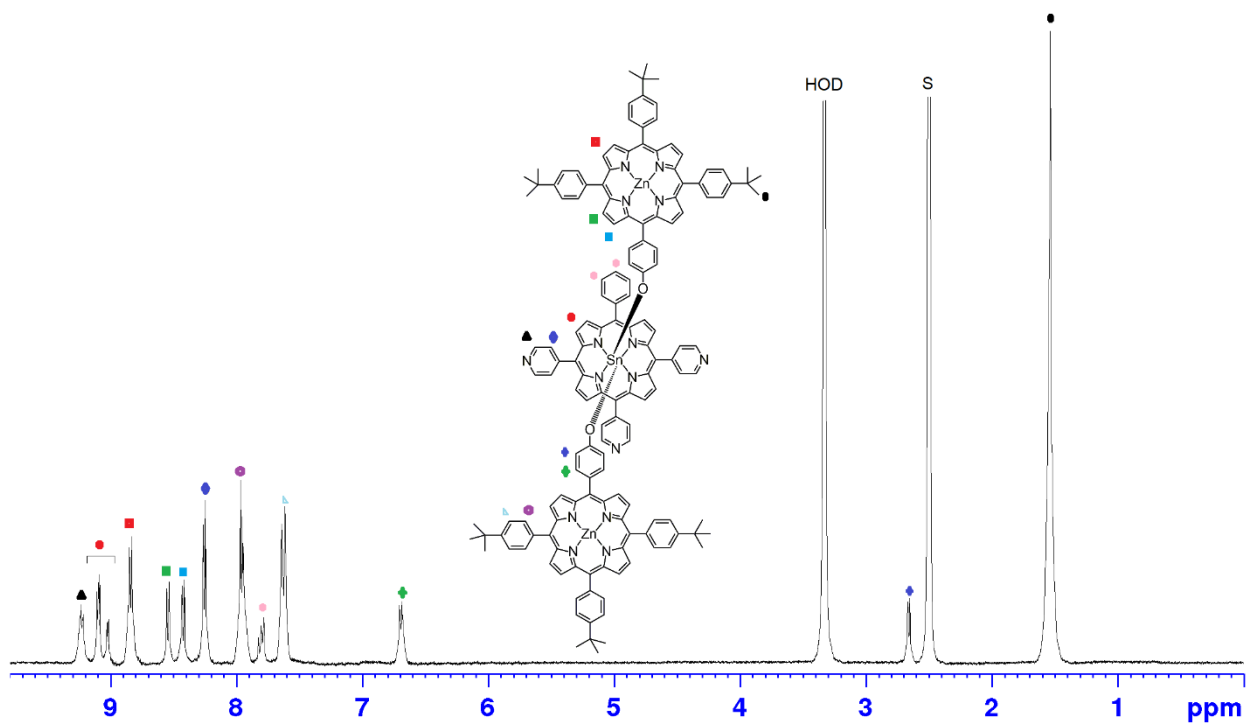


Fig. S5  $^1\text{H}$  NMR spectrum of triad **5** in  $\text{DMSO-d}_6$ .

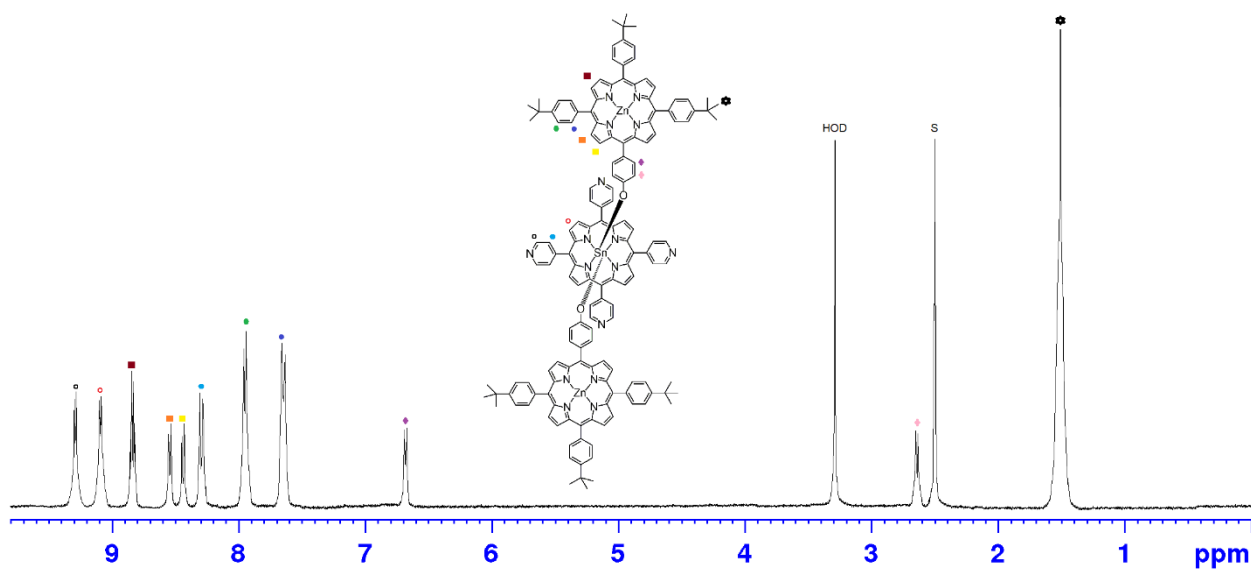
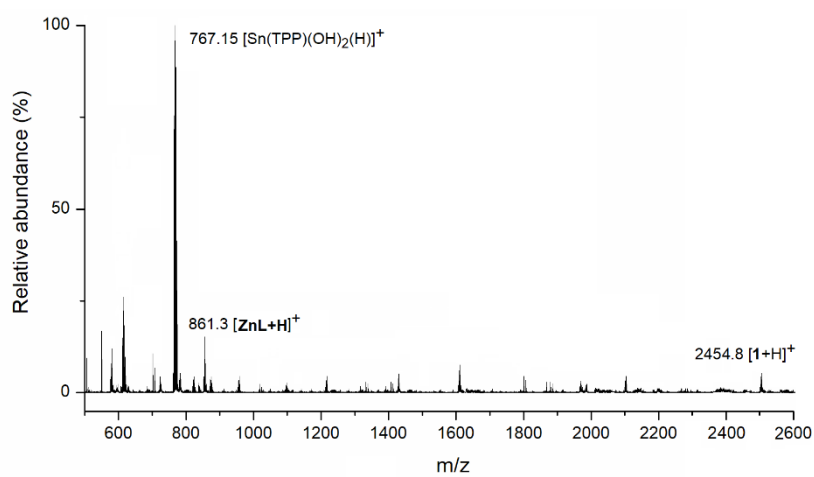
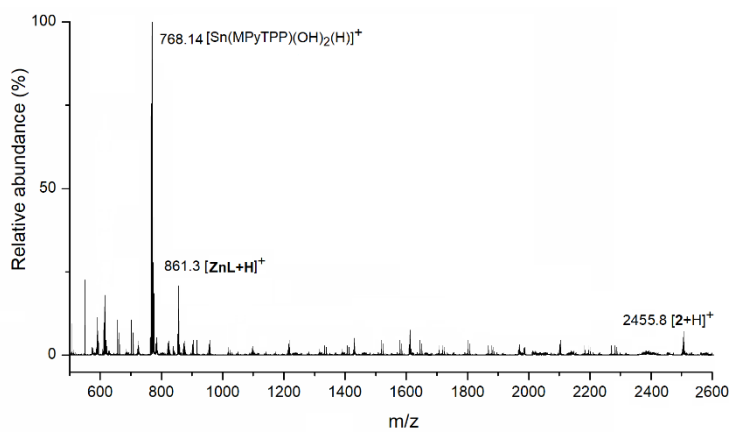


Fig. S6  $^1\text{H}$  NMR spectrum of triad **6** in  $\text{DMSO-d}_6$ .



**Fig. S7** ESI-mass spectrum of triad 1.



**Fig. S8** ESI-mass spectrum of triad 2.

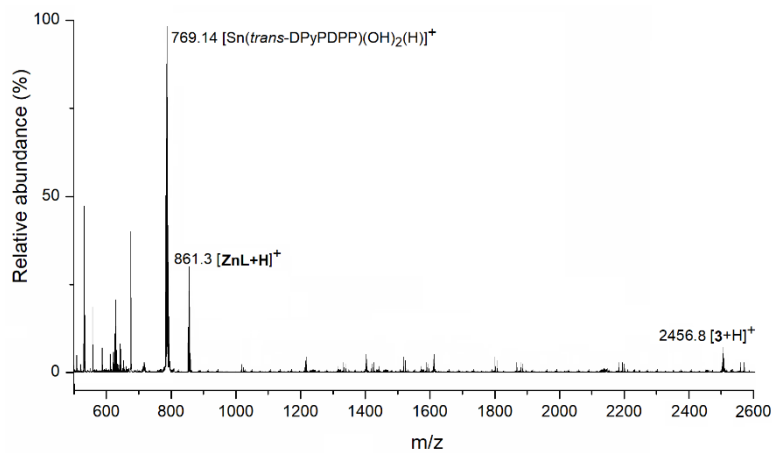


**Fig. S9** ESI-mass spectrum of triad 3.

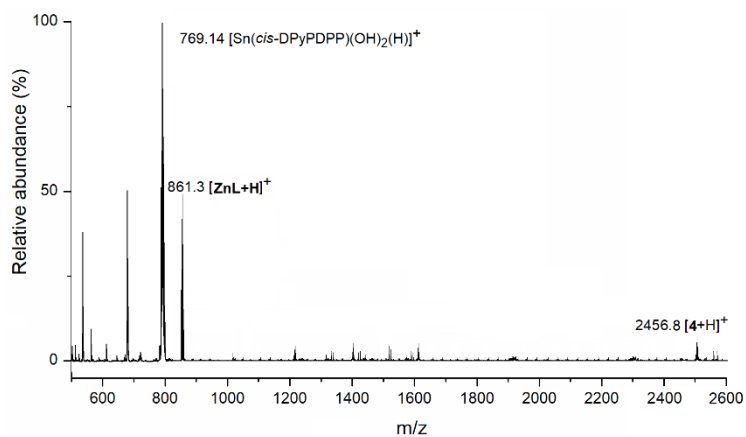


**Fig. S10** ESI-mass spectrum of triad 4.

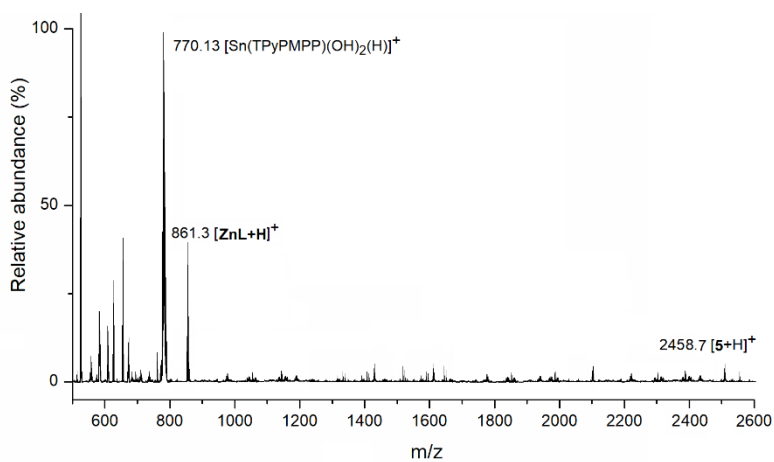


**Fig. S11** ESI-mass spectrum of triad 5.

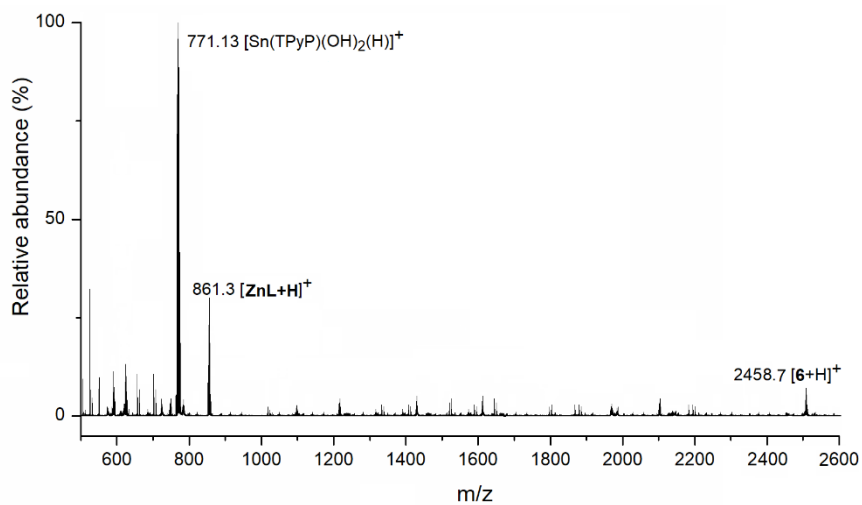


**Fig. S12** ESI-mass spectrum of triad 6.

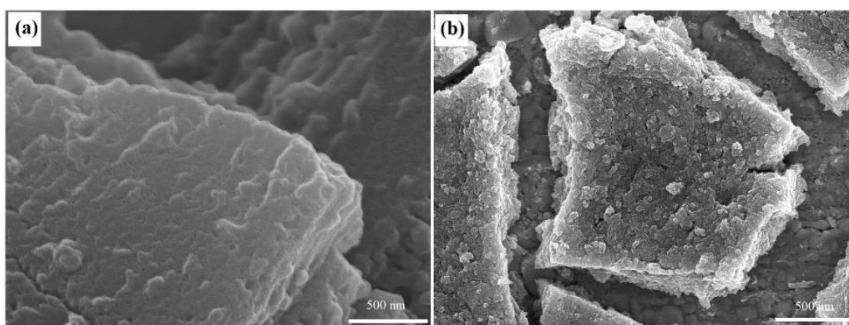


**Fig. S13** High-resolution FE-SEM images of the morphologies for self-assembled aggregates formed from the mixed solvent (toluene: *n*-hexane = 1:1). (a) ZnP; (b) SnP<sup>1</sup>.

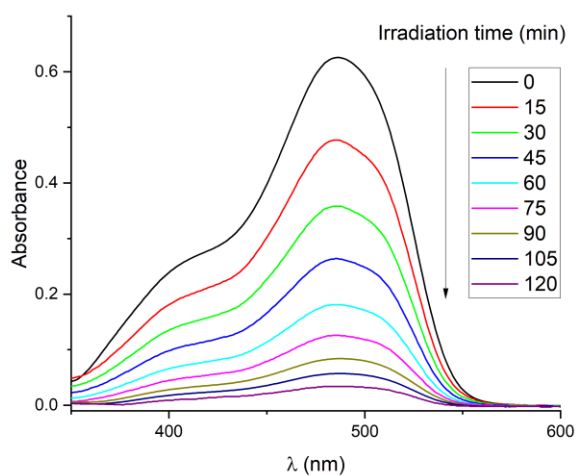


**Fig. S14** Time-dependent absorption spectra of Orange II (ORII) in the presence of photocatalyst derived from triad **4** under visible-light irradiation.

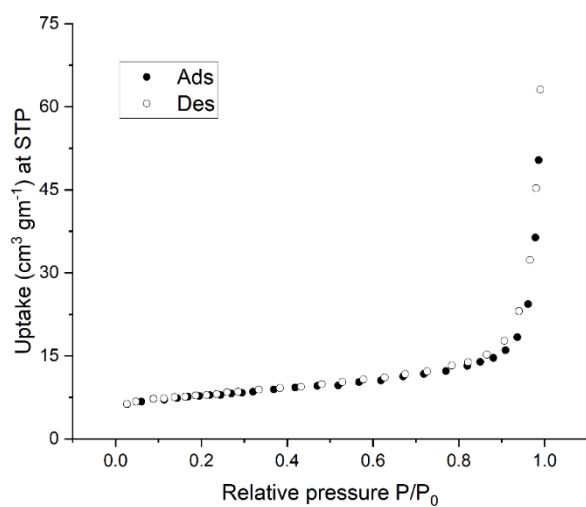


**Fig. S15** Adsorption and desorption isotherms of N<sub>2</sub> for catalyst **4** at 77 K.



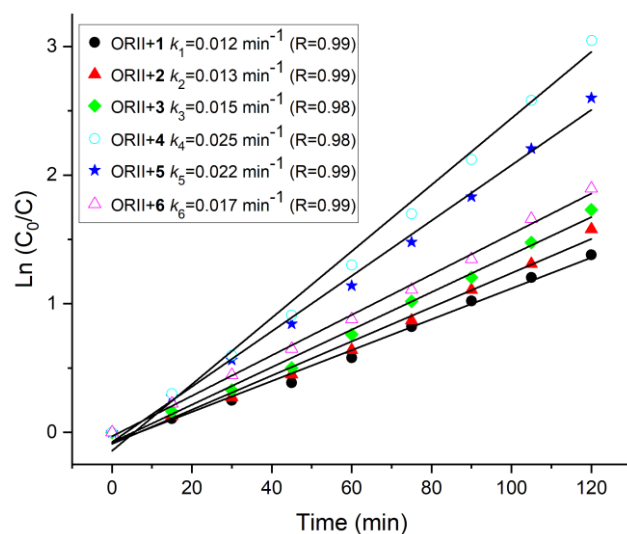


**Fig. S16** Kinetics for the photocatalytic degradation of Orange II (ORII) by nanostructures derived from mixed solvent system under visible-light irradiation.

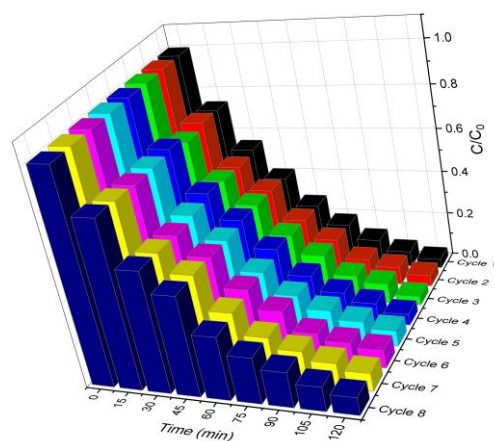


**Fig. S17** Catalytic cycles (consecutive 8 cycles) for photocatalyst **4** for the degradation of Orange II (ORII).

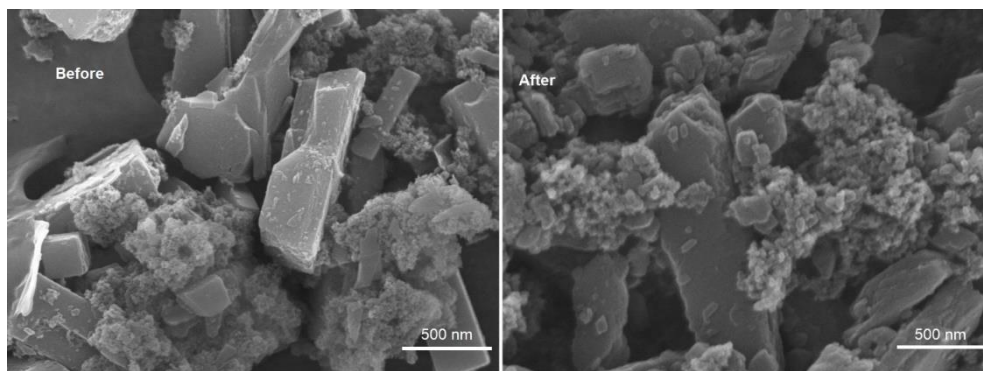


**Fig. S18** FE-SEM image of photocatalyst **4** after 8 consecutive cycles in the degradation of Orange II (ORII).

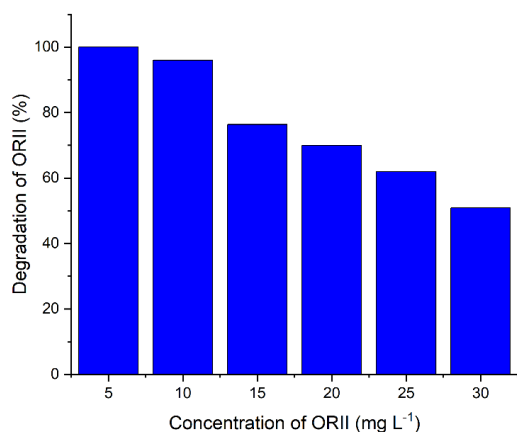


**Fig. S19** Performance of photocatalyst **4** (10 mg used) with respect to changes in initial concentration of Orange II (ORII).

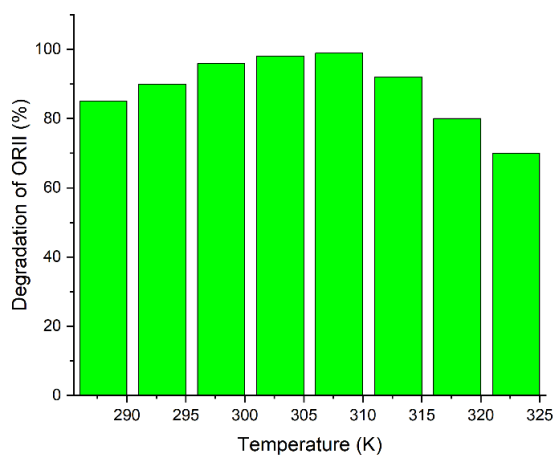


**Fig. S20** Effect of temperature for the degradation by photocatalyst **4**.

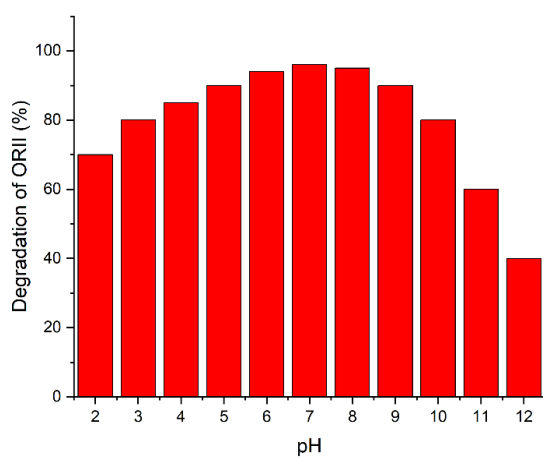


**Fig. S21** Effect of pH of the solution for the degradation by photocatalyst **4**.

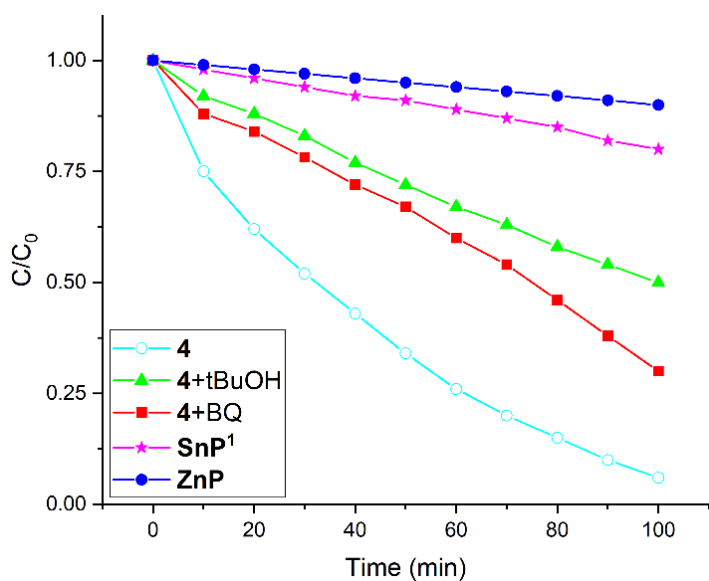


**Fig. S22** Photocatalytic degradation of Orange II (ORII) in aqueous solution by photocatalyst **4** generated from mixed solvent with the addition of different scavengers under visible light irradiation. **SnP<sup>1</sup>** and **ZnP** were also used as a catalyst for comparison.

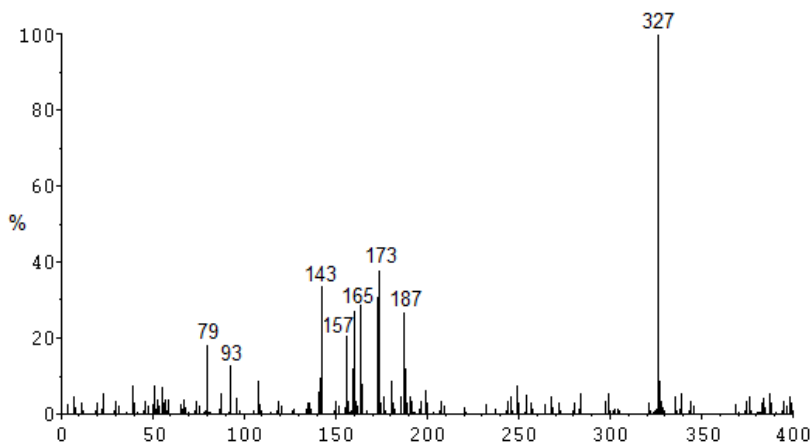


**Fig. S23** ESI-mass spectrum (negative ion mode) of the reaction mixture of Orange II (ORII) with photocatalyst **4** after 1 h of visible-light irradiation.